Available online at www.sciencedirect.com
ScienceDirect
Polymer 48 (2007) 3226–3236
polymer
www.elsevier.com/locate/polymer

Structure, phase transition and electric properties of poly(vinylidene fluoride-trifluoroethylene) copolymer studied with density functional theory

Zhi-Yin Wang [a], Hui-Qing Fan [a,**], Ke-He Su [b,*], Xin Wang [b], Zhen-Yi Wen [c]

[a] *State Key Laboratory of Solidification Processing, School of Materials Science and Engineering, Northwestern Polytechnical University, Xi'an, Shaanxi 710072, PR China*

[b] *School of Natural and Applied Sciences, Northwestern Polytechnical University, Xi'an, Shaanxi 710072, PR China*

[c] *Institute of Modern Physics, Northwest University, Xi'an, Shaanxi 710068, PR China*

Received 25 November 2006; received in revised form 2 April 2007; accepted 11 April 2007
Available online 18 April 2007

Abstract

The geometry, energy, internal rotation, vibrational spectra, dipole moments and molecular polarizabilities of poly(vinylidene fluoride-trifluoroethylene) (P(VDF-TrFE)) of α- and β-chain models were studied with density functional theory at B3PW91/6-31G(d) level and compared with those of the poly(vinylidene fluoride) (PVDF) homopolymer. The chain length and the trifluoroethylene (TrFE) concentration were examined to discuss the copolymer chain stabilities, chain conformations and electric properties. The asymmetrical internal-rotation potential energy curve shows that the angles for the *g* and *g*′ conformations in the α-chain (*tg* and *tg*′) models are 53° and −70°, respectively, and the β-chain (*ttt*) conformation is a slightly distorted *all-trans* plane with dihedral angle at 177°. The energy differences, $E_\beta - E_{\alpha(g)}$ and $E_\beta - E_{\alpha(g')}$, between the β- and the α-conformation are 2.1 and 7.8 kJ/mol, respectively. These values are smaller than that in PVDF (8.4 kJ/mol), suggesting that the β-conformation in the copolymer will be more stable than in PVDF. The energy barriers for $\beta \rightarrow \alpha(g)$ and $\beta \rightarrow \alpha(g')$ transitions are 16.2 and 5.8 kJ/mol, respectively. The former is almost twice of the energy barrier in PVDF by 8.2 kJ/mol and the latter is slightly smaller (by 2.4 kJ/mol) than that in PVDF. The respective energy barriers for $\alpha(g) \rightarrow \beta$ and $\alpha(g') \rightarrow \beta$ transitions are 18.3 and 13.6 kJ/mol compared with the value 16.3 kJ/mol in PVDF. The asymmetrical energy barriers may be one of the reasons for the copolymers with 0.5–0.6 (mole fraction) VDF exhibiting complicated phase transition behavior. The conformation of α-chain P(VDF-TrFE) exhibits from a *helical* (containing higher TrFE) to a nearly beeline (containing lower TrFE). This behavior is different from that in the PVDF and the nearly beeline conformation might be responsible for the increasing crystallizability. The *helical* might also be associated with the complicated phase transition behavior and the larger lattice strain in the P(VDF-TrFE)s with higher TrFE concentration. The energy difference per monomer unit between the β- and α-chain decreases with increasing TrFE content. The ideal β-chain is curved with a radius of about 30 Å, which is similar to that in PVDF. The chain curvature and the TrFE content will affect the dipole moment contribution per monomer. The chain length and TrFE content will not significantly affect the mean polarizability. The calculations indicated that there are some additional characteristic vibrational modes that may be used in identification of the α- or β-phase P(VDF-TrFE)s with different TrFE contents.

Keywords: DFT; P(VDF-TrFE); Polymer physical chemistry

1. Introduction

The discovery of the enhancement of piezoelectric activity in poly(vinylidene fluoride) (PVDF) by Kawai [1] led to the revelations of other properties, e.g., pyroelectricity [2,3] and ferroelectricity [4]. The exploration of the chemistry, physics, and technology of PVDF led to the search for other classes of novel ferroelectric polymers, such as its copolymers [5–8],

* Corresponding author. Tel.: +86 29 88493915; fax: +86 29 88493325.
** Corresponding author. Tel./fax: +86 29 88494463.
E-mail addresses: hqfan3@163.com (H.-Q. Fan), sukehe@nwpu.edu.cn (K.-H. Su).

0032-3861/$ - see front matter © 2007 Elsevier Ltd. All rights reserved.
doi:10.1016/j.polymer.2007.04.015

odd numbered polyimides [9,10], cyanopolymers [11,12], polyurethane [13,14], etc. Significant progresses in new materials and the understanding of structure–property relationships have been reported in the last decades.

Although PVDF possesses strong piezoelectric and pyroelectric properties, it is necessary that the polymer film be subjected to mechanical stretching and electrical poling to obtain the polar β-phase with the extended planar zigzag (*all-trans*) conformation. Such procedures include, for example, subjecting ferroelectric polymer to mechanical deformation [15,16], electron irradiation [17], uniaxial drawing [18], crystallization under high pressure [19] and crystallization under high electric field [20,21]. It is desirable to obtain a polymer with piezoelectric phase by simple treatment. Some improvements have been achieved by synthesizing copolymers of vinylidene fluoride (VDF) with trifluoroethylene (TrFE) [7,22–25], tetrafluoroethylene (TeFE) [23,26,27], vinyl fluoride (VF), or VDF/TrFE/chloro-containing terpolymers [28]. The copolymers were demonstrated to possess ferroelectricity over a wide composition range [29,30].

Compared with VDF, TrFE has lower polarity and TeFE does not have. However, the P(VDF-TrFE) and P(VDF-TeFE) copolymer systems can be grown with 90% or higher crystallinity [31–35], which results in stronger polarization and piezoelectric responses than those of the 50% crystalline PVDF. In addition, these structures can be grown in the form of ultrathin films [36,37] and have other important electromechanical properties, e.g., giant electrostriction [38,39]. Among these copolymers, the mostly studied system is the copolymer, poly(vinylidene fluoride-trifluoroethylene), obtained by random copolymerization of VDF and TrFE. This is also the best known and the most widely used ferroelectric polymer [40,41]. The randomly distributed VDF and TrFE units form the co-crystalline phase in the whole composition range. The larger proportion of bulky trifluorine atoms in the PVDF prevents the molecular chains from accommodating the α-chain (or $tgtg'$, where *g* refers *gauche* and *t* refers *trans*, and a prime ($'$) in *g* refers the dihedral angle being opposite to the *g* conformation with respect to the reference plane *t*) conformation. Therefore, the copolymer crystallizes directly at room temperature into a ferroelectric β-phase (or *ttt*, where *t* also refers *trans*) [42,43] that possesses a polar unit cell (similar to the β-phase of PVDF homopolymer), and the copolymer can be electroprocessed into a piezoelectric material immediately after crystallization.

The ferroelectric regions, with crystalline order, in the copolymer are embedded in an amorphous matrix. A number of experimental techniques and theoretical methods, such as differential scanning calorimetry, dielectric constant, ferroelectric measurement, X-ray diffraction, molecular dynamic (MD) simulation and *ab initio* technique, have been employed to investigate the electrical properties and structure changes during the phase transition of P(VDF-TrFE) to clarify the essential features of the transition mechanisms [23,24,44–47] and the origin of ferroelectric properties. The transition is associated with three types of crystalline phases, namely, the low-temperature (*LT*) phase, high-temperature (*HT*) phase and the cooled (*CL*) phase [40,44–51] and will be mainly affected by several factors, e.g., the composition of copolymer, history of heating, distribution of molecular weights and preparation conditions. Among those, the VDF content is especially important [40,50,52]. For instance, a copolymer sample with 0.7–0.8 (mole fraction) of VDF shows a clear and discontinuous first-order transition between the *LT* and *HT* phases at temperature close to the melting point [49,53]. A sample with 0.5–0.6 (mole fraction) of VDF, however, shows more complicated transition behavior [30,40,45,49,50,52,54]. In addition, experimental results show that the diffuse phase transition of copolymer from the ferroelectric into the paraelectric phase is also associated with the statistical variation of the VDF content of the crystallites [55]. Interestingly, there is a large strain change associated with the phase transformation. For example, for a copolymer with VDF/TrFE of 65/35 (mole ratio), the lattice strain as high as 10% has been detected during the phase transition [54].

In understanding the structure–property relationship of P(VDF-TrFE), Holman and Kavarnos [56] investigated the structural characteristics of amorphous and annealed P(VDF-TrFE) copolymers with VDF/TrFE of 50/50 (mole ratio) by molecular dynamics. Their MD computations predicted that the extent of *gauche*-character for PVDF is greater than that of its copolymer with 0.5 (mole fraction) of TrFE, at both high temperatures and after annealing. PVDF is enriched in *gauche*-conformations upon cooling, whereas the copolymer is enriched in *trans*-conformations. Farmer et al. [6], using potential energy calculations to determine the chain conformation and packing energies, confirmed that conversion between the α- and β-phase should be energetically feasible, and that increased concentration of head-to-head defects ($-CH_2$ refer to head and $-CF_2$ refer to tail) or TeFE co-monomer can cause the β-phase to become the favored structure for PVDF. From intermolecular potential investigations of P(VDF-TrFE), Lando and Doll [5] concluded that the isomorphous replacement of fluorine atoms by hydrogen atoms, which occurs in the head–head units in the homopolymer, strongly influences the polymorphism displayed by PVDF. Abe et al. [24] studied the phase transition of copolymer P(VDF-TrFE)s (with 0.5 and 0.7 mole fraction of VDF) by MD simulations. They predicted that the copolymer with higher VDF content exhibits the transition at higher temperature, and the molecular conformation in the high-temperature phase was a statistical combination of *tg*, tg', *tttg* and $tttg'$ sequences, in which the population of *tg* and tg' was higher and that of *tttg* and $tttg'$ was lower for the copolymer with higher VDF content. Nakhmanson et al. [23] investigated the polar properties of the β-phase of PVDF and its copolymers with TrFE and TeFE using an *ab initio* multigrid-based total-energy method. Their calculations show that polarization in such polymers is described by cooperative, quantum-mechanical interactions between polymer chains, which cannot be viewed as a superposition of rigid dipoles. For β-PVDF, the monomer dipole moment is increased by 50% (from 2 to 3 Debye) as the isolated chains are brought together to form a crystal. In PVDF crystals containing copolymers, they observed a weakly parabolic

dependence of monomer dipole moments on copolymer concentration.

However, there are still a number of questions remain unclear. For example, how will the magnitude of dipole moment per monomer unit change? How will the dipole moment per monomer unit contribute to the total dipole moment with increasing chain length? What will be the conformation of the chain with increasing copolymer chain length and TrFE content? Why the copolymer with high TrFE content shows complicated phase transition behavior? How will the TrFE content affect the phase transition behavior and electrical properties of the copolymer? Why the copolymers exhibit higher crystallinity than the homopolymer? From molecular structure point of view, the chain composition, conformation as well as energy difference of different phases are the important factors that affect the electrical properties and phase transition behavior of P(VDF-TrFE). Since the electrical properties originated from the crystal units, the chain orientation by stretching, crystallization by annealing, and CF_2 dipole orientation by poling are important in achieving high piezoelectric and pyroelectric constants. Also because the dipole orientation and magnitude are determined by chain conformation, chain packing, crystallinity and crystal size [57], it is interesting to investigate in detail how the VDF content alters the conformation and energy of a copolymer and, specifically, what role the VDF variety would play in the polymorphism of P(VDF-TrFE).

Since the VDF (or TrFE) concentration of the copolymer can be readily controlled by altering the molar ratio of VDF or TrFE in the generation of the copolymer models, this work will thus explore the structure and energy implications in increasing VDF content in P(VDF-TrFE) copolymers with the first principle method to answer most of the above questions. Internal rotation potentials, geometries and electrical properties of *tgtg′* and *all-trans* chains of P(VDF-TrFE) will be examined. For different conformations, energy differences, permanent dipole moment, mean polarizability per monomer and vibrational spectra will be analyzed. Some characteristic vibrational modes of α- and β-chain, which might be helpful in identification of the α- and β-phase P(VDF-TrFE)s, will be assigned and compared with experiments.

2. Theoretical method

Density functional theory (DFT), due to its feature of including the electronic correlation in a computationally efficient manner, has been used in larger molecular systems triumphantly [58–66]. In our previous systematic comparisons [67,68], a number of theoretical methods including DFT at BPW91, B3LYP and B3PW91 levels of theory, second order Møller–Plesset perturbation theory (MP2), and quadratic configuration interaction at QCISD and QCISD(T) levels with basis sets ranging from 6-31G(d,p), to 6-311G(2d,p) levels have been examined for geometry optimizations for all of the first and second row inorganic molecules collected in the CRC handbook of chemistry and physics [69]. It was shown that B3PW91 reproduces the equilibrium structures systematically better than the other methods with the same basis sets. We therefore employed B3PW91 (a combination of the Becke's three-parameter (B3) exchange functional [70,71] and the correlation functional of Perdew and Wang, PW91 [72]) in the present study. To balance accuracy and computational cost, 6-31G(d) (valence double ξ plus d polarization functions on heavy atoms) basis sets were chosen. The GAUSSIAN-03 package [73] was used for all of the calculations. We did not use p polarization functions for hydrogen atoms so that we can use the established frequency-scaling factor [74] in the spectrum analysis. The theoretical method employed in the current work is the same as that in Ref. [75] on PVDF for the convenience of further comparisons. Calculations were carried out on internal rotation potentials (of H[(CH_2CF_2)–($CHFCF_2$)]H dimer model), geometry optimizations, vibration analyses as well as molecular energies and dipole moment vectors (μ_x,μ_y,μ_z) of P(VDF-TrFE) for both α- and β-chain with different VDF contents and with different chain lengths in the models of H–[(CH_2CF_2)–($CHFCF_2$)]$_m$–H, H–[(CH_2CF_2)$_2$–($CHFCF_2$)]$_m$–H, H–[(CH_2CF_2)$_3$–($CHFCF_2$)]$_m$–H and H–[(CH_2CF_2)$_4$–($CHFCF_2$)]$_m$–H. Those models are for the ideal arrangement of alternating copolymers for simplifying the calculations. The clearly reported alternating piezoelectric copolymer was seen only in vinylidene cyanide with a number of other co-monomers [76,77]. Although the reported piezoelectric P(VDF-TrFE)s were the random copolymers, it is reasonable that there must have a higher proportion of alternating arrangement in the material as our models. For frequency analyses, the exact molecular polarizability tensors, $\alpha_{xx}^{\mathrm{mol}}$, $\alpha_{xy}^{\mathrm{mol}}$, $\alpha_{yy}^{\mathrm{mol}}$, $\alpha_{xz}^{\mathrm{mol}}$, $\alpha_{yz}^{\mathrm{mol}}$ and $\alpha_{zz}^{\mathrm{mol}}$, were obtained. The tensor, e.g., $\alpha_{xy}^{\mathrm{mol}}$, is defined as the linear response to an externally applied electric field [78]

$$\mu_x^{\mathrm{ind}} = \alpha_{xy}^{\mathrm{mol}} E_y^{\mathrm{ext}}$$

where μ^{ind} is the induced molecular dipole moment, E^{ext} is the magnitude of the applied electric field and x,y,z represent the Cartesian components. For vibrational analyses, the B3PW91/6-31G(d) frequencies were scaled by the scaling factor 0.9573 from Ref. [74].

3. Results and discussion

3.1. Internal rotation of dimer copolymer

Internal rotation of a polymer chain is the key step in phase transitions. Investigation with the dimer model of P(VDF-TrFE), H[(CH_2CF_2)–($CHFCF_2$)]H, was carried out to emphasize the intramolecular interactions. The internal rotation potential curve is plotted in Fig. 1(A), in which the curve of PVDF H[(CH_2CF_2)]$_2$H [75] is also plotted for comparison (Fig. 1(B)). The rotation begins and ends up at C–C–C–C *cis*-conformation (denoted as zero or 360° for the C–C–C–C dihedral angle). In Fig. 1(A), the conformation of the terminal $-CH_3$ group is determined by geometry optimizations without any restriction. The terminal $-CF_2H$ group is arranged to satisfy the conformation being the β-form (*all-trans*) when the C–C–C–C dihedral angle is 180°. The results show

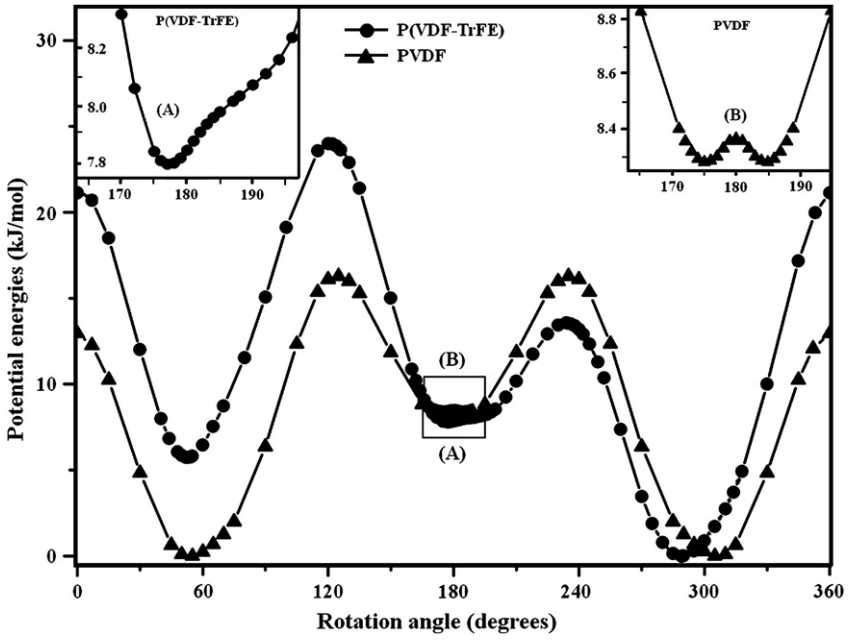

Fig. 1. Internal rotation potential energy curves of P(VDF-TrFE) and PVDF [75] chain units from H(CH_2CF_2)−($CHFCF_2$)H and H(CH_2CF_2)−(CH_2CF_2)H models obtained by B3PW91/6-31G(d) calculations.

that both the terminal groups are in staggered conformation with respect to the nearest (directly bonded) −CF_2 and −CHF segments.

Since four of the segments are different, the curve in Fig. 1(A) is not symmetric, which is different from the symmetric form in PVDF. This leads to the α-form having different conformational angles in the *tg* and *tg′* models. The value for *g* conformation is 53° and that for *g′* is −70° (or 290°). The respective results in the PVDF dimer are ±55°. It is shown in Fig. 1(A) that the most stable β-conformation in P(VDF-TrFE) will be a slightly distorted *all-trans* plane with dihedral angle at 177°, and that in PVDF is 2° farther from 180° i.e., at ±175° [75]. Therefore, the β-P(VDF-TrFE) copolymer will be more close to the ideal β-chain (the dihedral angle being 180°) conformation. However, as shown in Fig. 1(A) and compared with PVDF, the *all-trans* "ideal β-chain conformation" of P(VDF-TrFE) is no longer a transition state.

In the dimer model of P(VDF-TrFE), it is clear that the *tg′* conformation is more stable than *tg* by 5.7 kJ/mol. The energy differences, $E_\beta - E_{\alpha(g)}$ and $E_\beta - E_{\alpha(g')}$, between the β- and the α-conformation are 2.1 and 7.8 kJ/mol, respectively. Each of them is smaller than the value in PVDF (8.4 kJ/mol). This suggests that the β-conformation in the copolymer will be more stable compared with PVDF thermodynamically.

The energy barriers for $\beta \rightarrow \alpha(g)$ and $\beta \rightarrow \alpha(g')$ transitions are 16.2 and 5.8 kJ/mol, respectively. The former is almost twice of the energy barrier in PVDF by 8.2 kJ/mol, but the latter is slightly (with 2.4 kJ/mol) smaller than that in PVDF. The respective energy barriers for $\alpha(g) \rightarrow \beta$ and $\alpha(g') \rightarrow \beta$ transitions are 18.3 and 13.6 kJ/mol compared with 16.3 kJ/mol in PVDF. The complexities of the energy barriers may be one of the reasons for the copolymers with 0.5−0.6 (mole fraction) of VDF exhibiting complicated phase transition behavior as has been found in the experiments [30–35,40,45,49,50,52,79,80]. The present result also predicts that the low-energy $\alpha(g')$ conformation should be dominant (more or less) in the α-phase obtained either from preparation or from depolarization of β-phase in the copolymers.

3.2. Structure and stability

In order to explore the structure and stability of P(VDF-TrFE) copolymers with different components, structures of α- (*tgtg′*) and β-chain (*ttt*) within 2−*n* (*n* = 20 or 21) monomer units in the models of H−[(CH_2CF_2)−($CHFCF_2$)]$_m$−H ($n = 2m$), H−[(CH_2CF_2)$_2$−($CHFCF_2$)]$_m$−H ($n = 3m$), H−[(CH_2CF_2)$_3$−($CHFCF_2$)]$_m$−H ($n = 4m$) and H−[(CH_2CF_2)$_4$−($CHFCF_2$)]$_m$−H ($n = 5m$) were optimized and compared with those of PVDF [75]. The mole fractions of VDF are 0.50, 0.67, 0.75 and 0.80, and the β-chain is for the ideal conformation in these models. The third fluorine atom of TrFE in the copolymer is arranged alternately with respect to the chain axis in simulating the most probable orientation of TrFE in the polymerization reactions. It is interesting that the alternate arrangement of the third fluorine atom of TrFE may not be the most stable structure as has been found in an extra examination in the α-model of H−[(CH_2CF_2)−($CHFCF_2$)]$_2$−H, where an additional segment went into the more stable *g′* conformation, leading to an energy lower by 4.1 kJ/mol for each monomer unit. However, the alternate arrangement should be more reasonable for the most probable orientation of TrFE in the practical reactions.

The optimized structures at B3PW91/6-31G(d) level for the models with 20 or 21 monomer units are shown in Fig. 2(a)–(h). For the ideal β-conformation copolymers, all of the chains are curved. It is interesting that the β-chain P(VDF-TrFE)

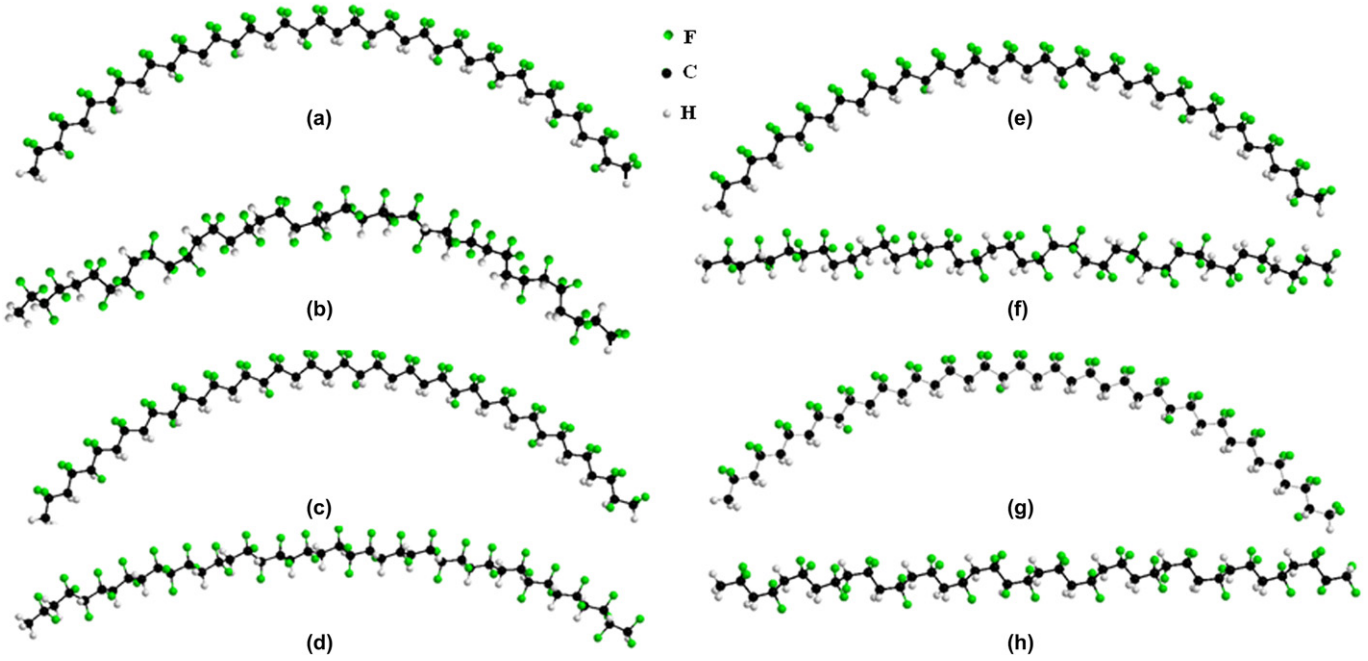

Fig. 2. Optimized structures of P(VDF-TrFE) by B3PW91/6-31G(d) calculations: (a) and (b) are for β- and α-chain with 20 monomers containing 0.50 mole fraction of VDF in H−[(CH_2CF_2)−($CHFCF_2$)]$_m$−H; (c) and (d) are for β- and α-chain with 21 monomers containing 0.67 mole fraction of VDF in H−[(CH_2CF_2)$_2$−($CHFCF_2$)]$_m$−H; (e) and (f) are for β- and α-chain with 20 monomers containing 0.75 mole fraction of VDF in H−[(CH_2CF_2)$_3$−($CHFCF_2$)]$_m$−H; (g) and (h) are for β- and α-chain with 20 monomers containing 0.80 mole fraction of VDF in H−[(CH_2CF_2)$_4$−($CHFCF_2$)]$_m$−H.

containing different VDF ratios has almost the same curvature radii of 29−30 Å. It is quite similar to the β-chain PVDF homopolymer [75]. This is an unexpected result for the copolymers since it would be expected that increasing of the ratio of TrFE (having more F atoms to balance the number of F atoms on both sides of the chain axis) would have reduced the curvature of β-chains. However, it remains almost unchanged. In fact, the enriched F models have a little smaller average curvature radii of 29.10, 29.66, 29.71 and 29.83 Å for the chains containing 0.50, 0.33, 0.25 and 0.20 mole fractions of TrFE, respectively. This could be explained that the alternant electrostatic attraction between the negative F atom and the neighboring positive H atom increased as shown in Fig. 2(a). The smaller chain curving for the chains having smaller TrFE ratio is understandable by electrostatic interactions as what in PVDF [75]. That is the electrostatic repulsion between F atom couples being on the outer side of the chain with less (or without in PVDF) attraction on the inner side, and consequently the radius is the largest by 30.31 Å for the 20-monomer PVDF [75].

Compared with the arched α-PVDF homopolymer [75], the copolymer chain containing 0.50 mole fraction of TrFE (Fig. 2(b)) is clearly in a *helical* structure other than a planar curve. The chains having 0.25 (Fig. 2(f)) and 0.20 (Fig. 2(h)) mole fractions of TrFE are nearly in beeline, and the chain with 0.33 (Fig. 2(d)) mole fraction of TrFE is in between. It is well known that the beeline polymer chain has higher crystalline order and is in favor of forming crystals or larger crystals to achieve a high crystallinity. Since all of the β-chain copolymers are curved (in the same curvature as the homopolymer PVDF, implying that the β-chain copolymers would not be responsible for enhancing crystallinity), it is therefore that the nearly beeline α-chain copolymer results in higher crystallinity. Consequently the highly crystallized copolymer can be electroprocessed into the piezoelectric β-phase.

Compared with that in PVDF, the α → β transition in P(VDF-TrFE) with high TrFE might have an additional process of releasing the *helical* chain (with higher TrFE content in *tgtg′* monomer order) into beeline structure (with *ttt* monomer order). The complexity of this process might result in complicated phase transition behavior as has been found in the experiments [30−35,40,45,49,50,52,79,80]. The helical releasing process would also have larger chain deformations, leading to larger lattice strain as that has been observed in the phase transition of P(VDF-TrFE) copolymer with 0.65 mole fraction of VDF [54].

Fig. 3 plots the energy differences per monomer unit between the α- and β-chain, i.e., $(E_\beta - E_\alpha)/n$, vs. chain lengths. The VDF concentration in Fig. 3(a)−(d) is 0.50, 0.67, 0.75 and 0.80 (mole fractions) for the copolymer chains containing 2 to n ($n \leq 21$) monomer units. Fig. 3(e) shows the energy difference of PVDF homopolymer [75] for comparison. It is clear that the energy difference in the homopolymer increases with increasing chain length and converges to a nearly constant value of 10 kJ/mol. The energy difference in the copolymer with a constant concentration also converges to a nearly constant value with increasing chain length for $n \geq 8$. However, the value is smaller than that in PVDF. For the models having different TrFE concentrations in Fig. 3(a)−(d), the energy differences increase with decreasing TrFE content. The average values for $n \geq 8$ are listed in Table 1. These are 4.1, 5.5, 7.0 and 8.3 kJ/mol for Fig. 3(a)−(d) compared with 10.0 kJ/mol for PVDF.

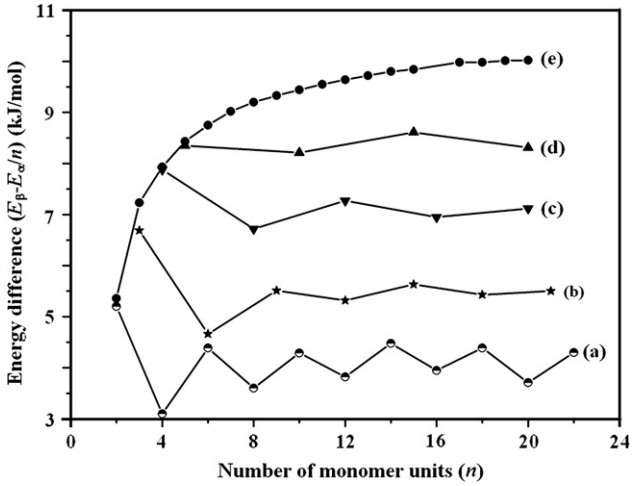

Fig. 3. Energy differences per monomer unit between the α- and β-chain: $(E_\beta - E_\alpha)/n$, vs. chain lengths obtained from B3PW91/6-31G(d): (a) copolymer, H−[(CH$_2$CF$_2$)−(CHFCF$_2$)]$_m$−H, $n = 2m$; (b) copolymer, H−[(CH$_2$CF$_2$)$_2$−(CHFCF$_2$)]$_m$−H, $n = 3m$; (c) copolymer, H−[(CH$_2$CF$_2$)$_3$−(CHFCF$_2$)]$_m$−H, $n = 4m$; (d) copolymer, H−[(CH$_2$CF$_2$)$_4$−(CHFCF$_2$)]$_m$−H, $n = 5m$; (e) From Ref. [75] for homopolymer, H−[(CH$_2$−CF$_2$)$_n$]−H.

It is interesting that the energy differences for the copolymers converge in zigzag ways within an energy range of about 0.5 kJ/mol. The energy oscillation is from the unbalanced F atoms beside the chain plane of β-conformation as shown in Fig. 4, as an example. The lower energy cases correspond to Fig. 4(a) with balanced F atoms, which will not yield additional bending force onto the chain plane. But for the case of Fig. 4(b), three F atoms are below the plane and two are above. This leads to an additional bending force onto the plane from the negative F atoms attracting the neighboring positive H atoms. However, we forced the plane un-bended in the calculations of the ideal β-chains leading to the slightly higher energies.

The lowest energy difference per monomer unit shown in Table 1 is 4.1 kJ/mol in the 0.50 mole fraction TrFE copolymer compared with the highest one 10 kJ/mol [75] in the

Table 1
Magnitude of the energy differences per monomer unit between the α- and β-chain for different VDF contents in the P(VDF-TrFE) copolymer and the contribution magnitude of dipole moment per monomer unit in the β-chain P(VDF-TrFE) containing different VDFs obtained from B3PW91/6-31G(d) calculations

VDF content in the P(VDF-TrFE)/mole fractions	0.50[a]	0.67[b]	0.75[c]	0.80[d]	1.00[e]
$(E_\beta - E_\alpha)/n$ (kJ/mol)	4.1	5.5	7.0	8.3	10.0
Contribution of dipole moment per unit[f]/10^{-30} C m	3.75	4.27	4.48	4.68	5.31
Contribution of dipole moment per unit[g]/10^{-30} C m	3.52	3.98	4.26	4.41	5.10

[a] P(VDF-TrFE), H−[(CH$_2$CF$_2$)−(CHFCF$_2$)]$_m$−H.
[b] P(VDF-TrFE), H−[(CH$_2$CF$_2$)$_2$−(CHFCF$_2$)]$_m$−H.
[c] P(VDF-TrFE), H−[(CH$_2$CF$_2$)$_3$−(CHFCF$_2$)]$_m$−H.
[d] P(VDF-TrFE), H−[(CH$_2$CF$_2$)$_4$−(CHFCF$_2$)]$_m$−H.
[e] PVDF H−[(CH$_2$−CF$_2$)$_n$]−H, homopolymer from Ref. [75].
[f] Chains with 15 monomer units, data are derived from Fig. 5.
[g] Chains with 20 monomer units, data are derived from Fig. 5.

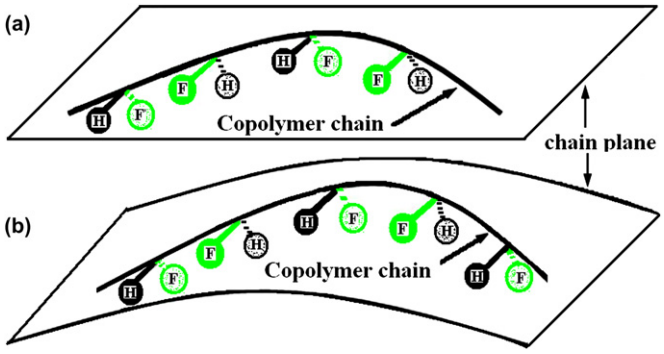

Fig. 4. Illustration of ideal β-chain P(VDF-TrFE) with balanced and unbalanced F atoms beside the chain plane that leads to the oscillations of energy differences in Fig. 3. The VDF units and CF$_2$ segments of TrFE are not shown in the figure. Bonds with solid lines are above the plane and those with dashed lines are below the plane. (a) Number of F atoms are identical on both sides and (b) more F atoms are below the chain plane attracting the neighboring positive H atoms in CH$_2$ segments, leading to chain plane bending.

PVDF homopolymer. The results show that the introduction of TrFE into VDF is in favor of forming *trans*-conformation copolymer (or β-phase). This might be the reason that the copolymers are able to crystallize into ferroelectric β-phase at room temperature but PVDF homopolymer is not [42,43]. Obviously, the decrease of energy of β-chain and the decrease of curvature of α-chain (Fig. 2(b), (d), (f) and (h)) by TrFE copolymerization are propitious to form ferroelectric β-phase and to increase crystallinity as has been observed in experiments [31–35,42,43].

3.3. Dipole moment and mean polarizability

Determined by conformation, stability of molecular aggregate, electric dipole and polarizability, the electric response properties are of fundamental importance in piezoelectricity copolymers. Since a typical copolymer contains molecular chains with some statistical distribution of lengths, and in order to examine the chain length and VDF content affecting the electrical properties of P(VDF-TrFE), we have calculated the average permanent dipole moment per monomer unit $\mu = (\mu_x^2 + \mu_y^2 + \mu_z^2)^{1/2}/n$ and the mean polarizabilities per monomer unit $\alpha = (\alpha_{xx} + \alpha_{yy} + \alpha_{zz})/3n$ [78] for different chain lengths (with n units) and different VDF contents as shown in Figs. 5 and 7.

Similar to β-PVDF [75], the dipole moment contribution per monomer unit decreases with increasing chain length for the β-chain P(VDF-TrFE)s (Fig. 5). This is because the dipole moment from the individual monomer unit is perpendicular to the chain but the β-chain is curved. For the β-P(VDF-TrFE), the decreased magnitude, −1.24%, of dipole moment contribution per monomer unit is similar to that of PVDF (i.e., −1.2% per monomer [75]). This is consistent with the fact that P(VDF-TrFE) has almost the same curvature radii as the β-chain PVDF discussed previously. However, for the P(VDF-TrFE)s with higher TrFE content, the absolute values of the dipole moments decreased. This is because the −(CHFCF$_2$)− segment in TrFE has lower dipole moment (2.60×10^{-30} C m [23]) than −(CH$_2$CF$_2$)− in VDF

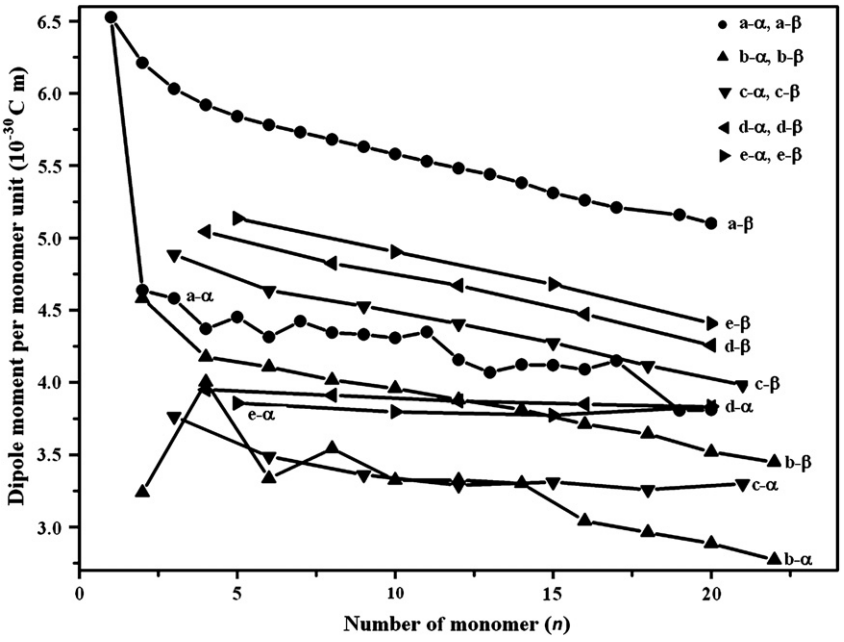

Fig. 5. Dipole moment per monomer unit vs. P(VDF-TrFE) chain length: (a-β) and (a-α) are for β- and α-chain PVDFs from Ref. [75]; (b-β) and (b-α) are for β- and α-chain P(VDF-TrFE)s containing 0.50 mole fraction of VDF; (c-β) and (c-α) are for β- and α-chain P(VDF-TrFE)s containing 0.67 mole fraction of VDF; (d-β) and (d-α) are for β- and α-chain P(VDF-TrFE)s containing 0.75 mole fraction of VDF; (e-β) and (e-α) are for β- and α-chain P(VDF-TrFE)s containing 0.80 mole fraction of VDF.

(6.53×10^{-30} C m [75], 6.67×10^{-30} C m [23]). For the 15- and 20-monomer copolymer chains, the typical numerical results are listed in Table 1.

For the α-chain P(VDF-TrFE)s, it is shown that the overall dipole moment contribution per monomer unit decreases with increasing chain lengths for the copolymer with 0.50 mole fraction of VDF (Fig. 5(b-α)). However, the values are not always evenly decreased mainly due to the complexity of the *helical* structure. For the chains containing 0.67–0.80 mole fractions of VDF (Fig. 5(c-α), (d-α) and (e-α)), each of the values is nearly a constant for the reason that the chains are almost in beeline.

The magnitude of dipole moment contributed per monomer unit in β-P(VDF-TrFE) with 15- and 20-monomer units with respect to the VDF content is plotted in Fig. 6. The figure shows that the dipole moment per monomer unit increases rapidly with increasing VDF content. This is because the dipole moment in VDF is larger. The curve is nearly in a linear relation, but there exists a very weakly parabolic dependence of dipole moment per monomer on VDF concentration. This behavior is similar to the results of PVDF copolymers predicted by *ab initio* multigrid-based total-energy method [23]. A fit to the curve provides an estimate of the contributed magnitude of dipole moment per monomer unit (in 10^{-30} C m) in the β-chain P(VDF-TrFE) at any VDF molar fraction x in the range between 0.50 and 1.00. The linear and quadratic fittings are (with the correspondence correlation coefficient R in the parentheses):

$$\mu_{(15\ \text{monomer})} = 2.182 + 3.116x \quad (R = 0.99928)$$

$$\mu_{(20\ \text{monomer})} = 1.896 + 3.172x \quad (R = 0.99843)$$

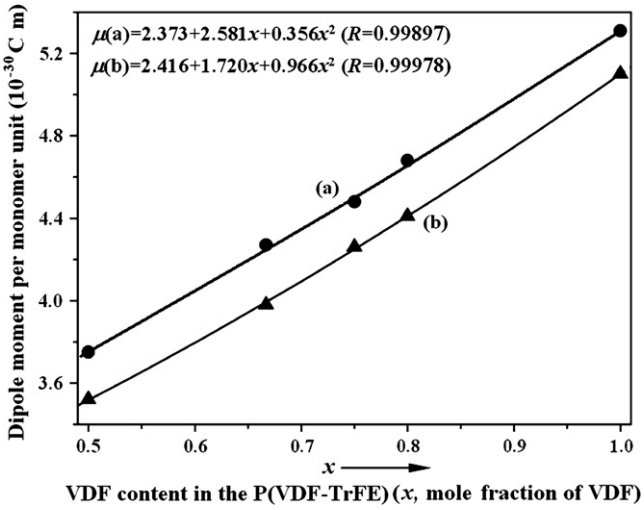

Fig. 6. Dependence of magnitudes of dipole moment contributed per monomer unit on VDF content (x, molar fraction) in the β-chain P(VDF-TrFE) obtained from B3PW91/6-31G(d) calculations: (a) 15-monomer model; (b) 20-monomer model.

$$\mu_{(15\ \text{monomer})} = 2.373 + 2.581x + 0.356x^2 \quad (R = 0.99897)$$

$$\mu_{(20\ \text{monomer})} = 2.416 + 1.720x + 0.966x^2 \quad (R = 0.99978)$$

The quadratic fit is slightly better than the linear. As has been found in Ref. [23], where the authors did not give any explanation, the very weakly parabolic dependence appears again in this work. A possible explanation is that the chain curvature slightly decreases with increasing VDF content (as discussed in Section 3.2) leading to the slight increase in dipole moment contribution.

For the β-chain P(VDF-TrFE) containing two units (i.e., H−(CH_2CF_2)−($CHFCF_2$)−H), the contribution magnitude of dipole moment is 4.58×10^{-30} C m as shown in Fig. 5(b-β) if the chain curvature can be neglected. This is consistent with the prediction of *ab initio* multigrid-based total-energy method ($(2.0 + 0.78)/2$ Debye $= 4.64 \times 10^{-30}$ C m) [23]. Although the contribution magnitude of the dipole moment per monomer unit decreases with increasing chain length, the total dipole moment of chain increases with increasing chain length. For the 10- and 20-monomer copolymer chains, for example, the values (in 10^{-30} C m) are 39.6 and 70.4 (with 0.50 mole fraction of VDF), 44.8 and 80.6 (with 0.67 mole fraction of VDF), 47.5 and 85.1 (with 0.75 mole fraction of VDF), 49.1 and 88.1 (with 0.80 mole fraction of VDF), respectively. Therefore, the β-P(VDF-TrFE) copolymer with longer chain and with higher VDF has higher piezoelectric and pyroelectric properties.

Fig. 7 shows that the mean polarizability per monomer unit in β-chain P(VDF-TrFE) is slightly higher than that in α-chain P(VDF-TrFE). Chain length does not significantly affect the mean polarizability of either α- or β-P(VDF-TrFE). For the β-chain P(VDF-TrFE)s with different VDF contents, the mean polarizabilities per monomer unit are in a small range of $3.61-3.64 \times 10^{-40}$ C m^2 V^{-1}. The sequence in the models is $0.50 > 0.67 > 0.75 > 0.80$ (mole fraction of VDF). A similar sequence is also found in the α-chain P(VDF-TrFE)s with the mean polarizabilities in the range of $3.56-3.69 \times 10^{-40}$ C m^2 V^{-1}.

3.4. Vibrational spectra

It is interesting to examine the properties associated with the changes of the chain conformation and crystalline structure by introducing TrFE in the polymer. The infrared spectrum is one of the most important tools to examine the changes. The IR vibrational spectra for both α- and β-chain P(VDF-TrFE)s with 5−16 monomer units containing different molar ratios of VDF were obtained. Some of the results within the wavenumber 400−1500 cm^{-1} are shown in Figs. 8 and 9. The figures have included the spectra of the PVDF homopolymer as a reference and the experimental spectra [28] of P(VDF-TrFE). Fig. 8(a) is the simulated spectra for the α-chain PVDF homopolymer having 15 monomer units [75], (b)−(e) are for the α-chain P(VDF-TrFE)s copolymer having 15 (12 or 14) monomer units with different VDF contents, and (f) is a experimental spectra of the copolymer with 0.55 mole fraction of VDF [28]. Fig. 9(a) is the simulated spectra for the β-chain PVDF having 15 monomer units [75], (b)−(e) are for the β-chain P(VDF-TrFE)s having 15 (or 16) monomer units with different VDF contents, and (f) is also the experimental spectra of copolymer with 0.55 mole fraction of VDF as in Fig. 8(f) [28]. The same image of the experimental spectra is employed in Fig. 9, because it has been analyzed in Ref. [28] that the spectra are for a sample containing both α- and β-phase.

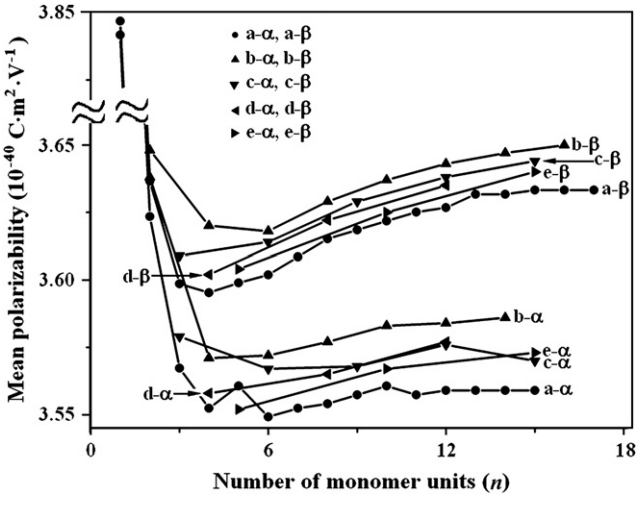

Fig. 7. Mean polarizability per monomer unit vs. the length of the copolymer chains: (a-β) and (a-α) are for β- and α-chain PVDFs from Ref. [75]; (b-β) and (b-α) are for β- and α-chain P(VDF-TrFE)s containing 0.50 mole fraction of VDF; (c-β) and (c-α) are for β- and α-chain P(VDF-TrFE)s containing 0.67 mole fraction of VDF; (d-β) and (d-α) are for β- and α-chain P(VDF-TrFE)s containing 0.75 mole fraction of VDF; (e-β) and (e-α) are for β- and α-chain P(VDF-TrFE)s containing 0.80 mole fraction of VDF.

Comparison shows that the calculated spectra of the α-chain P(VDF-TrFE)s with different VDF contents are similar to that of the α-chain homopolymer PVDF [75] (Fig. 8(a)). The spectra are also very close to the experimental spectra [28] (Fig. 8(f)). The most distinguishable vibrational modes are found in the signature region. The peaks at 546 and 700 cm^{-1} are the modes mainly from the $-CH_2$ and $-CF_2$ rocking and skeletal bending. These two peaks were not found in the homopolymer PVDF [75]. It has also seen that the intensities of the peaks at 546 and 700 cm^{-1} increase with increasing TrFE content in the copolymer P(VDF-TrFE). The frequencies of α-PVDF at 590 and 739 cm^{-1} (CF_2 bending and skeletal bending) [81] shift to the higher wavenumbers (i.e., from 594 to 598 cm^{-1} and from 747 to 766 cm^{-1}) in the α-P(VDF-TrFE) with increasing TrFE content. It should be noted that most of the theoretical signature peaks were not shown in the experimental spectra. This might be from the insufficient chain length in the theoretical models or from the lack of intermolecular interaction consideration for condensed sample or from the insufficient resolution of the experiments or even from the other complexities affecting the observations as presented in Ref. [75].

Fig. 9 shows the IR spectra of the β-chain P(VDF-TrFE)s with different VDF contents. The spectra are also similar to those of the β-chain PVDF (Fig. 9(a)). Compared with those of the α-chain, the spectra of the β-chain P(VDF-TrFE) are more close to the experiments (Fig. 9(f) from Ref. [28]). This suggests that the β-phase is dominant in the copolymer sample. The most distinguishable vibrational modes are found for the peaks in 1030−1111 cm^{-1} (Fig. 9(e)). These peaks correspond to the modes mainly from the C^{FH}−F (where C^{FH} refers to the C atom bonding F and H atoms) stretching, CFH scissoring, and $-CH_2$ rocking and twisting. It is interesting that the peaks were not found in the homopolymer PVDF [75] except for the sole intense peak at 1029 cm^{-1}, which gradually disappeared and shifted to higher frequencies. The intensities of the peaks in 1030−1111 cm^{-1} increase with

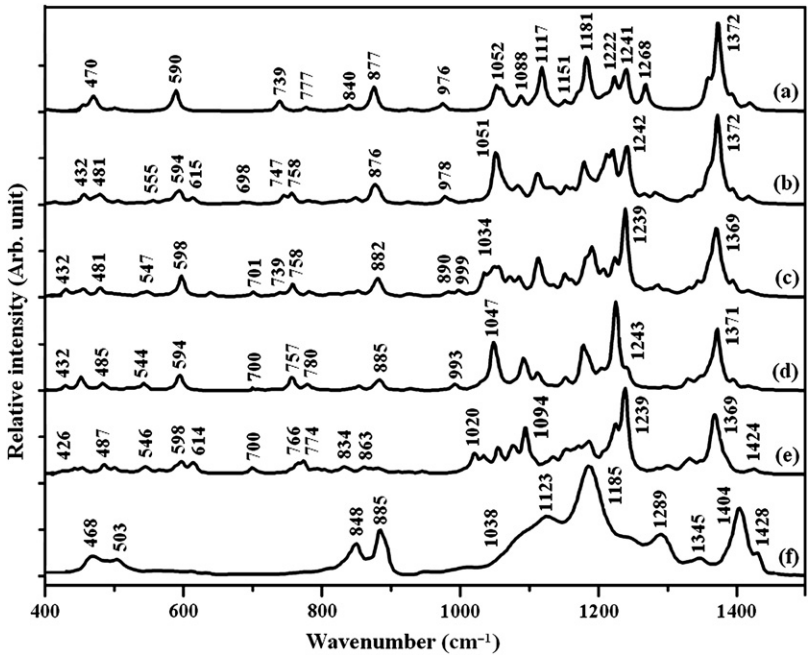

Fig. 8. Comparison of the IR spectra of α-chain P(VDF-TrFE)s with different TrFE contents (obtained by B3PW91/6-31G(d) calculations): (a) PVDF with 15 monomer units (from Ref. [75]. Here we correct a mistake made in the spectra (Figs. 8–10) in Ref. [75], where the labeled theoretical wavenumbers had not been scaled by the scaling factor 0.9573, which is not consistent with the text of that paper. The present labels are the scaled values.); (b) P(VDF-TrFE) with 15 monomer units containing 0.80 mole fraction of VDF; (c) P(VDF-TrFE) with 12 monomer units containing 0.75 mole fraction of VDF; (d) P(VDF-TrFE) with 15 monomer units containing 0.67 mole fraction of VDF; (e) P(VDF-TrFE) with 14 monomer units containing 0.50 mole fraction of VDF; (f) experimental spectra of P(VDF-TrFE) containing 0.55 mole fraction of VDF (from Ref. [28]).

increasing TrFE content. The intensity of the characteristic vibrational peak of β-PVDF at 840 cm^{-1} (CH_2 rocking [81–83] and all of the $-CH_2$ groups collectively and symmetrically moving in-plane and perpendicular to the polymer chain [75]) slightly increases with increasing TrFE content. Other intense characteristic peaks of β-PVDF at 1224 cm^{-1} (CF_2

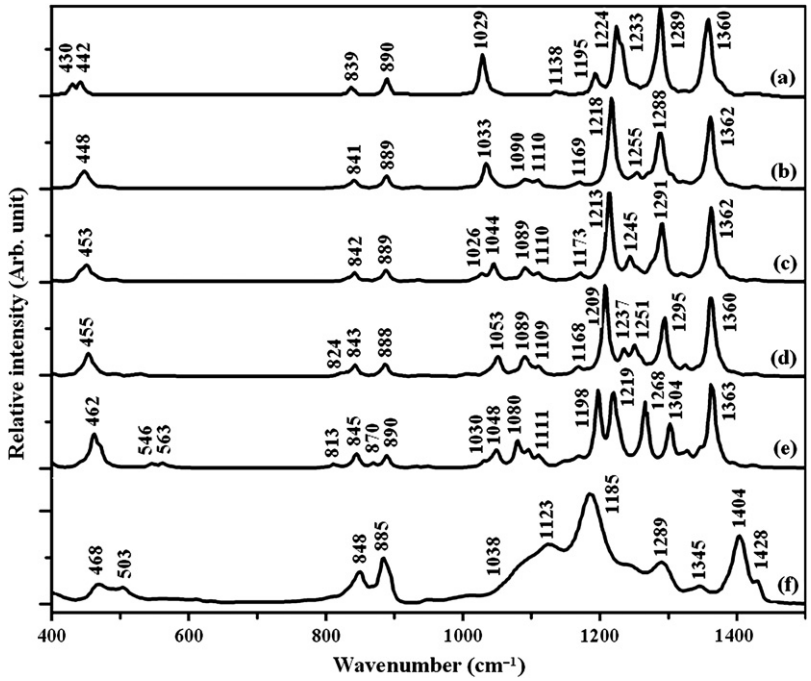

Fig. 9. Simulated IR spectra of β-chain PVDF and P(VDF-TrFE) from B3PW91/6-31G(d) calculations: (a) PVDF with 15 monomer units (from Ref. [75]); (b) P(VDF-TrFE) with 15 monomer units containing 0.80 mole fraction of VDF; (c) P(VDF-TrFE) with 12 monomer units containing 0.75 mole fraction of VDF; (d) P(VDF-TrFE) with 15 monomer units containing 0.67 mole fraction of VDF; (e) P(VDF-TrFE) with 16 monomer units containing 0.50 mole fraction of VDF; (f) experimental spectra of P(VDF-TrFE) containing 0.55 mole fraction of VDF (from Ref. [28]).

out-of-plane deformation [82,84,85]) and 1233 cm^{-1} [75] broadens and shifts to lower wavenumbers (1198 and 1219 cm^{-1}) with increasing TrFE content in P(VDF-TrFE). These results might be used for identification of the α- and β-P(VDF-TrFE).

4. Conclusions

In this study, DFT-B3PW91/6-31G(d) has been employed to investigate the internal rotation potentials, geometries, relative stabilities, vibrational spectra, dipole moments and mean polarizabilities of the α- and β-chain P(VDF-TrFE)s with different TrFE contents. Chain length and TrFE (or VDF) content related to the electric properties and vibrational spectra have been discussed. The following are conclusions drawn from the present theoretical calculations.

1. The internal rotation potential of the $H(CH_2CF_2)-(CHFCF_2)H$ model shows that the angles for the *g* and *g′* conformations in the α-chain (*tg* and *tg′*) model are 53° and −70° (compared with PVDF, the values are ±55°), and that the β-chain (*ttt*) is a slightly distorted *all-trans* plane with the dihedral angles at 177°, which are more close to an ideal β-conformation. The energy differences, $E_\beta - E_{\alpha(g)}$ and $E_\beta - E_{\alpha(g')}$, between the β- and the α-conformation are 2.1 and 7.8 kJ/mol, respectively and are smaller than the value in PVDF (8.4 kJ/mol). This suggests that the β-conformation in the copolymer will be more stable thermodynamically. The energy barriers for $\beta \rightarrow \alpha(g)$ and $\beta \rightarrow \alpha(g')$ transitions are 16.2 and 5.8 kJ/mol, respectively. The former is larger and the latter is smaller than the energy barrier 8.2 kJ/mol in PVDF. The respective energy barriers for $\alpha(g) \rightarrow \beta$ and $\alpha(g') \rightarrow \beta$ transitions are 18.3 and 13.6 kJ/mol compared with 16.3 kJ/mol in PVDF. The complexities of the energy barriers may be one of the reasons why the copolymers with 0.5–0.6 mole fraction of VDF exhibit complicated phase transition behavior. The low-energy $\alpha(g')$ conformation is predictive of the dominant conformation in the α-phase copolymers.
2. All of the ideal β-chain P(VDF-TrFE)s with 6–20 (or 6–21) monomer units and with different VDF contents are curved into an almost same radius as PVDF (about 30 Å). In the α-chain P(VDF-TrFE)s, however, copolymer chains exhibit a *helical* form (containing 0.50 mole fraction of TrFE) to a nearly beeline (containing 0.20–0.25 mole fraction of TrFE) with increasing VDF content. The *helical* form of α-chain P(VDF-TrFE) (with higher TrFE content) might be related to the complicated phase transition behaviors and the larger lattice strain. The chain in the beeline form (with lower TrFE content) might be responsible for increasing crystallinity and crystal size.
3. The energy difference for the copolymer P(VDF-TrFE) with a constant composition converges to a nearly constant value with increasing chain length. The energy difference decreases with increasing TrFE content in the copolymer P(VDF-TrFE). This result indicted that the copolymerization of VDF with TrFE is in favor of stabilizing the *trans*-conformation.
4. The energy decrease of β-chain with increasing TrFE content in the copolymer and the decrease of α-chain curvature with increasing VDF content in the copolymer are propitious to form ferroelectric β-phase. This is also helpful to understand why copolymers are able to crystallize into a ferroelectric β-phase at room temperature but PVDF homopolymer is not.
5. The decreased magnitude of dipole moment contribution per monomer unit, for the β-chain P(VDF-TrFE) with a constant VDF content, is similar to that of PVDF (i.e., −1.2% per monomer in the β-chain PVDF) due to similar chain bending. For the α- and β-chain P(VDF-TrFE)s with different VDF contents, the magnitude of dipole moment contribution per monomer unit decreases with increasing content of TrFE. This is because the VDF segment, $-(CH_2CF_2)-$, has higher dipole moment than TrFE, $-(CHFCF_2)-$. For a given chain length of P(VDF-TrFE), the dipole moment per monomer unit increases rapidly with increasing VDF content. The curve is nearly in a linear relation, but there exists a very weakly parabolic dependence of dipole moment per monomer on VDF concentration from the slightly difference of the curvature of the chains. Chain length does not show a significant change on mean polarizability for both of the α- and β-chain P(VDF-TrFE)s. The mean polarizability per monomer unit in β-chain is slightly higher than that in α-chain.
6. By comparing the calculated IR spectra of the α- and β-chain P(VDF-TrFE)s containing different VDF contents with those of PVDF, vibrational bands for the α- or β-P(VDF-TrFE) identifications are proposed.

Acknowledgements

This work was supported by the National Nature Science Foundation (Nos. 50572089, 50672075) and the Xi'an S&T Research Foundation (GG05015, GG06023). Part of the calculations was performed in the High Performance Computing Center of Northwestern Polytechnical University.

References

[1] Kawai H. Jpn J Appl Phys 1969;8:975–6.
[2] Bergman Jr JG, McFee JH, Crane GR. Appl Phys Lett 1971;18:203–5.
[3] Anderson RA, Kepler RG, Lagasse RR. Ferroelectrics 1981;33:91–4.
[4] Furukawa T, Date M, Fukada E. J Appl Phys 1980;51:1135–41.
[5] Lando JB, Doll WW. J Macromol Sci Phys 1968;2:205–33.
[6] Farmer BL, Hopfinger AJ, Lando JB. J Appl Phys 1972;43:4293–303.
[7] Yagi T, Tatemoto M, Sako JI. Polym J 1980;12:209–23.
[8] Yagi T, Tatemoto M. Polym J 1979;11:429–36.
[9] Lee JW, Ttakase Y, Newman BA, Scheinbeim JI. J Polym Sci Part B Polym Phys 1991;29:273–8.
[10] Lee JW, Ttakase Y, Newman BA, Scheinbeim JI. J Polym Sci Part B Polym Phys 1991;29:279–86.
[11] Stupp SI, Carr SH. Colloid Polym Sci 1979;257:913–9.
[12] Stupp SI, Carr SH. J Polym Sci Part B Polym Phys 1978;16:13–28.

[13] Cheng ZY, Gross S, Su J, Zhang QM. J Polym Sci Part B Polym Phys 1999;37:983–90.
[14] Zheyi M, Scheinbiem JI, Lee JW, Newman BA. J Polym Sci Part B Polym Phys 1994;32:2721–31.
[15] Tashiro K, Kobayashi M. Macromolecules 1988;21:2463–9.
[16] Tashiro K, Kobayashi M. Macromolecules 1990;23:2802–6.
[17] Lovinger AJ. Macromolecules 1985;18:910–8.
[18] Furukawa T, Seo N. Jpn J Appl Phys 1990;29:675–80.
[19] Yuki T, Ito S, Koda T, Ikeda S. Jpn J Appl Phys 1998;37:5372–4.
[20] Chung MY, Lee DC. J Korean Phys Soc 2001;38:117–22.
[21] Kepler RG, Anderson RA, Lagasse RR. Phys Rev Lett 1982;48:1274–7.
[22] Higashihata Y, Sako J, Yagi T. Ferroelectrics 1981;32:85–92.
[23] Nakhmanson SM, Buongiorno Nardelli M, Bernholc J. Phys Rev B 2005;72:115210.
[24] Abe Y, Tashiro K, Kobayashi M. Comput Theor Polym Sci 2000; 10:323–33.
[25] Hattori T, Watanabe T, Akama S, Hikosaka M, Ohigashi H. Polymer 1997;38:3505–11.
[26] Hicks JC, Jones TE, Logan JC. J Appl Phys 1978;49:6092–6.
[27] Lovinger AJ. Macromolecules 1983;16:1529–34.
[28] Petchsuk A. Ferroelectric terpolymers, based on semicrystalling VDF/ TrTE/Chloro-containing termonomers: synthesis, electrical properties, and functionalizations. The Pennsylvania State University; 2003. p. 97–126 [chapter 4].
[29] Tajitsu T, Chiba A, Furukawa T, Date M, Fukada E. Appl Phys Lett 1980;36:286–8.
[30] Tashiro K, Takano K, Kobayashi M, Chatani Y, Tadokoro H. Polymer 1981;22:1312–4.
[31] Furukawa T. IEEE Trans Electr Insul 1989;24:375–94.
[32] Tajitsu Y, Ogura H, Chiba A, Furukawa T. Jpn J Appl Phys Part 1 1987;26:554–60.
[33] Tasaka S, Miyata S. J Appl Phys 1985;57:906–10.
[34] Ohigashi H, Omote K, Gomyo T. Appl Phys Lett 1995;66:3281–3.
[35] Omote K, Ohigashi H, Koga K. J Appl Phys 1997;81:2760–9.
[36] Bune AV, Fridkin VM, Ducharme S, Blinov LM, Palto SP, Sorokin AV, et al. Nature 1998;391:874–7.
[37] Cai L, Qu HW, Lu CX, Ducharme S, Dowben PA, Zhang JD. Phys Rev B 2004;70:155411.
[38] Zhang QM, Bharti V, Zhao X. Science 1998;280:2101–4.
[39] Casalini R, Roland CM. J Polym Sci Part B Polym Phys 2002;40: 1975–84.
[40] Tashiro K. Crystal structure and phase transition of PVDF and related copolymers. In: Nalwa HS, editor. Ferroelectric polymers, series of plastic engineering. New York: Marcel Dekker; 1995.
[41] Lovinger AJ. Science 1983;220:1115–21.
[42] Balta Calleja FJ, Arche AG, Ezquerra TA, Cruz CS, Batallan F, Frick B, et al. Adv Polym Sci 1993;108:1–48.
[43] Ohigashi H, Akama S, Koga K. Jpn J Appl Phys 1988;27:2144–50.
[44] Tashiro K, Kobayashi M. Phase Transitions 1989;18:213–46.
[45] Davis GT, Furukawa T, Lovinger AJ, Broadhurst MG. Macromolecules 1982;15:329–33.
[46] Tashiro K, Tanaka R, Kobayashi M. Macromolecules 1999;32:514–7.
[47] Ploss B. Polymer 2000;41:6087–93.
[48] Lovinger AJ. In: Bassett DC, editor. Developments in crystalline polymers. New Jersey: Applied Science Publishers; 1998. p. 195.
[49] Lovinger AJ, Furukawa T, Davis GT, Broadhurst MG. Polymer 1983;24: 1225–32.
[50] Lovinger AJ, Furukawa T, Davis GT, Broadhurst MG. Polymer 1983; 24:1233–9.
[51] Lovinger AJ, Davis GT, Furukawa T, Broadhurst MG. Macromolecules 1982;15:323–8.
[52] Tashiro K, Takano K, Kobayashi M, Chatani Y, Tadokoro H. Polymer 1984;25:195–208.
[53] Yagi T, Higashihata Y, Fukuyama K, Sako J. Ferroelectrics 1984;57:327–35.
[54] Tashiro K, Takano K, Kobayashi M, Chatani Y, Tadokoro H. Ferroelectrics 1984;57:297–326.
[55] Legrand JF, Lajzerowicz J, Berge B, Delzenne P, Macchi F, Bourgaux-Leonard C, et al. Ferroelectrics 1988;78:151–8.
[56] Holman RW, Kavarnos GJ. Polymer 1996;37:1697–701.
[57] Kim KJ, Hsu SL. Polymer 1994;35:3612–8.
[58] Hutchison GR, Ratner MA, Marks TJ. J Phys Chem B 2005;109: 3126–38.
[59] Zhang JP, Frenking G. J Phys Chem A 2004;108:10296–301.
[60] Grozema FC, van Duijnen PT, Siebbeles LDA, Goossens A, de Leeuw SW. J Phys Chem B 2004;108:16139–46.
[61] Fratiloiu S, Grozema FC, Siebbeles LDA. J Phys Chem B 2005;109: 5644–52.
[62] Zhan CG, Nichols JA, Dixon DA. J Phys Chem A 2003;107: 4184–95.
[63] Hutter J, Luthi HP, Diederich F. J Am Chem Soc 1994;116:750–6.
[64] Li FF, Wu DS, Lan YZ, Shen J, Huang SP, Cheng WD, et al. Polymer 2006;47:1749–54.
[65] Yang L, Feng JK, Ren AM, Sun JZ. Polymer 2006;47:1397–404.
[66] Yang L, Feng JK, Ren AM, Sun CC. Polymer 2006;47:3229–39.
[67] Su KH, Wei J, Hu XL, Yue H, Lü L. Acta Phys Chim Sin 2000;16: 643–51.
[68] Su KH, Wei J, Hu XL, Yue H, Lü L. Acta Phys Chim Sin 2000;16: 718–23.
[69] Lide DR, editor. CRC handbook of chemistry and physics. 77th ed. CRC Press; 1996–1997. p. 9-15–9-23 (Editor in Chief).
[70] Becke AD. J Chem Phys 1992;97:9173–7.
[71] Becke AD. J Chem Phys 1993;98:5648–52.
[72] Burke K, Perdew JP, Wang Y. In: Dobson JF, Vignale G, Das MP, editors. Electronic density functional theory: recent progress and new directions. Plenum; 1998. p. 177–97.
[73] Frisch MJ, Trucks GW, Schlegel HB, Scuseria GE, Robb MA, Cheeseman JR, et al. Gaussian 03, Revision B.01. Pittsburgh: Gaussian, Inc; 2003.
[74] Scott AP, Radom L. J Phys Chem 1996;100:16502–13.
[75] Wang ZY, Fan HQ, Su KH, Wen ZY. Polymer 2006;47:7988–96.
[76] Conciatori AB, Trapasso LE, Stackman RW. In: Mark HF, editor. Encyclopedia of polymer science and technology, vol. 14. New York: John Wiley and Sons; 1971. p. 580.
[77] Furukawa T, Date M, Nakajima K, Kosaka T, Seo I. Jpn J Appl Phys 1986;25:1178–82.
[78] Solymar L, Walsh D. In: Oxford, editor. Lectures on the electric properties of materials. 4th ed. Oxford: Oxford University Press; 1989.
[79] Cheng SZD, Lotz B. Polymer 2005;46:8662–81.
[80] Lotz B, Cheng SZD. Polymer 2005;46:577–610.
[81] Salimi A, Yousefi AA. Polym Test 2003;22:699–704.
[82] Bocaccio T, Bottino A, Capanelli G, Piaggi P. J Membr Sci 2002;210: 315–29.
[83] Gregorio R, Capitao RC. J Mater Sci 2000;35:299–306.
[84] Wang CL, Li JC, Zhong WL, Zhang PL. Synth Met 2003;135–136: 469–70.
[85] Li JC, Wang CL, Zhong WL, Zhang PL, Wang QH, Webb JF. Appl Phys Lett 2002;81:2223–5.